

Photoelectron angular distributions in negative-ion photodetachment from mixed *sp* states

Emily R. Grumbling and Andrei Sanov^{a)}*Department of Chemistry and Biochemistry, University of Arizona, Tucson, Arizona 85721, USA*

(Received 15 August 2011; accepted 28 September 2011; published online 24 October 2011)

We describe an approach for constructing analytical models for the energy-dependence of photoelectron angular distributions in the one-electron, non-relativistic approximation. We construct such a model for electron emission from an orbital described as a superposition of *s*- and *p*-type functions, using linearly polarized light. In the limits of pure *s* or pure *p* electron photodetachment or photoionization, the model correctly reproduces the familiar Cooper–Zare formula. The model predictions are compared to experimental results for strongly solvated H^- and NH_2^- , corresponding to predominantly *s* and predominantly *p* character parent states, respectively. © 2011 American Institute of Physics. [doi:10.1063/1.3653234]

I. INTRODUCTION

Photoelectron imaging has become increasingly widespread in the study of gas-phase negative ions.¹ This technique^{2–4} yields both photoelectron energy spectra and the corresponding angular distributions from a single experiment. While interpretation of the photoelectron spectra in terms of binding energies, Franck–Condon overlap and relative energy levels of the corresponding neutral relies on routine methods of classic photoelectron spectroscopy,^{5,6} the process of extracting information from photoelectron angular distributions remains less developed.^{7–12}

For one-photon electron detachment or ionization with linearly polarized light, photoelectron angular distributions (PAD) have the general form:^{13–15}

$$I(\theta) = \frac{\sigma_{tot}}{4\pi} [1 + \beta(3 \cos^2 \theta - 1)/2], \quad (1)$$

where the anisotropy parameter β (ranging from -1 to 2) completely defines the PAD with respect to the direction of the electric field vector of the incident radiation. On a conceptual level, it is often convenient to consider photodetachment or photoionization under the one-electron approximation. In this case, the wave functions of all other electrons in the system are presumed unchanged and the transition dipole matrix elements are evaluated between the initial (bound) and the final (free) states of the one electron involved in the transition. One may also neglect interchannel interactions and relativistic effects. This picture is admittedly crude, yet it often captures, at a qualitative level, the essential physics—and chemistry—of the process.

According to the derivations by Bethe,¹⁶ generalized by Cooper and Zare,^{14,15} the anisotropy parameter for photodetachment or photoionization for an atomic system is given by the Cooper–Zare equation:

$$\beta = \frac{\ell_i(\ell_i - 1)\chi_{\ell_i, \ell_i-1}^2 + (\ell_i + 1)(\ell_i + 2)\chi_{\ell_i, \ell_i+1}^2 - 6\ell_i(\ell_i + 1)\chi_{\ell_i, \ell_i+1}\chi_{\ell_i, \ell_i-1} \cos(\delta_{\ell_i+1} - \delta_{\ell_i-1})}{(2\ell_i + 1)[\ell_i\chi_{\ell_i, \ell_i-1}^2 + (\ell_i + 1)\chi_{\ell_i, \ell_i+1}^2]}, \quad (2)$$

where ℓ_i is the orbital angular momentum quantum number of the parent orbital, $\chi_{\ell_i, \ell_i \pm 1}$ are the radial matrix elements for the dipole-allowed free-electron partial waves with $\ell = \ell_i \pm 1$, and $\delta_{\ell_i \pm 1}$ are the corresponding phase shifts induced by interactions with the remaining neutral species or cation.

In the particular case of photodetachment or photoionization from an *s* orbital ($\ell_i = 0$), Eq. (2) predicts a perfect $\beta = 2$, regardless of electron kinetic energy. Alternatively,

one may arrive at the same prediction by making use of the one-electron selection rule, $\Delta\ell = \pm 1$ and $\Delta m_\ell = 0$, to determine that the process should yield an outgoing *p* wave ($\ell = 1$), polarized the same way as the light source. Such a wave corresponds to a cosine-squared angular distribution, described by Eq. (1) with $\beta = 2$. This prediction is consistent with experimental observations for photodetachment from an *s* orbital.^{17–19} In photodetachment or photoionization from an atomic *p* orbital, photoelectron waves with $\ell = 0$ and 2 are allowed. The photoelectron wave function is a coherent

^{a)}Electronic mail: sanov@u.arizona.edu.

superposition of these waves and the resulting PAD is dependent on electron kinetic energy, ε . Although Eq. (2) does not contain ε explicitly, the dependence is realized through the radial matrix elements $\chi_{\ell_i, \ell_i \pm 1}$.

The Cooper–Zare equation (Eq. (2)) can be rearranged to show that β is dependent not on the matrix elements themselves, but the ratio of χ_{ℓ_i, ℓ_i+1} and χ_{ℓ_i, ℓ_i-1} . In anion photodetachment, this ratio is often expected to vary linearly with energy, as originally noted by Hanstorp *et al.*²⁰ This simplification can be deduced from the Wigner law²¹ for anion photodetachment, $\sigma_\ell \propto \varepsilon^{\ell+1/2}$, since the partial-wave cross sections (σ_ℓ) are proportional to the squares of the corresponding matrix elements, $\sigma_\ell \propto \chi_{\ell_i, \ell}^2$ ($\ell = \ell_i \pm 1$).

A common criticism concerning the use of the Wigner law proportionality over energy ranges spanning several electron-volts is that the law, being a *threshold* law, is strictly valid only at vanishingly small kinetic energies.^{21–24} However, decades of successful and diverse applications of Hanstorp *et al.*'s approach²⁰ appear to suggest that, while the Wigner law predictions of partial wave cross sections are not accurate outside the threshold regime, its predictions of cross section *ratios* probably are.^{10, 18, 25–39} Assuming $\sigma_{\ell_i+1}/\sigma_{\ell_i-1} \propto \varepsilon^2$ and, therefore, $\chi_{\ell_i, \ell_i+1}/\chi_{\ell_i, \ell_i-1} = A\varepsilon$, where A is a proportionality coefficient, Eq. (2) can be rearranged to allow the calculation of β as an explicit function of ε via the Wigner–Bethe–Cooper–Zare (WBCZ) equation:²⁰

$$\beta = \frac{\ell_i(\ell_i - 1) + (\ell_i + 1)(\ell_i + 2)A^2\varepsilon^2 - 6\ell_i(\ell_i + 1)A\varepsilon \cos(\delta_{\ell_i+1} - \delta_{\ell_i-1})}{(2\ell_i + 1)[\ell_i + (\ell_i + 1)A^2\varepsilon^2]}. \quad (3)$$

Photodetachment from molecular systems has been considered analogously, though with two notable differences. First, as ℓ is not a rigorous quantum number for non-atomic species, group theory has been used to identify all transition-dipole-allowed contributions to the photoelectron wave.^{24, 28} Second, the angle-resolved differential cross sections result from averaging over all orientations of the system with respect to the laboratory frame and, therefore, polarization direction of the incident radiation.^{13–15, 24, 40} In the absence of spherical symmetry, orientation averaging can be treated either exactly, by explicit integration, or approximately, by considering a limited number of symmetry-adapted “principal” orientations of the molecule in the laboratory frame.^{9, 10, 28, 41–43}

In many notable cases, it has been pointed out that the parent molecular orbital may be described as essentially an atomic s, p, or d-like function. For example, the chemistry of carbenes and the photodetachment of carbene anions are largely controlled by the non-bonding p (σ or π) orbitals on the central carbon atom.^{44–46} Similarly, the highest-occupied molecular orbital (HOMO) of O_2^- , a $\pi_g^*(2p)$ molecular orbital, is well described as a d-like function (effective $\ell_i = 2$).^{24, 37} However, in other cases a single function with defined ℓ_i value may not be sufficient, as for parent states that are best described as superpositions of two or more atomic-like orbitals. For example, describing the $\pi^*(2p)$ HOMO of the NO^- anion as a d-like molecular orbital is useful, but not as good an approximation as in the O_2^- case,³¹ while describing this HOMO as a sum of d and p functions would be more appropriate. Other important examples include hybrid orbitals and atomic orbitals perturbed by interactions with strong-solvent molecules, such as s or s-like states polarized by directional charge-dipole interactions.

Despite the developments in photoelectron imaging, there is no simple analogue of the Cooper–Zare central-potential model for cases of mixed-character states, where the parent orbital is represented as a linear combination of two (or

more) atomic-like functions with different ℓ_i values. In what follows, we take a step towards developing such a model and describe a non-perturbative analytic approach to photoelectron angular distributions for photodetachment or photoionization from an orbital of mixed character with linearly polarized light within the non-relativistic, one-electron picture.

In general terms, the angular component of the parent orbital—regardless of its identity—is expanded in the complete basis of the spherical harmonics (centered at a convenient point, not necessarily coinciding with any particular atom in the molecule). In our approach, orientation averaging inherent in the transformation from the molecular to the laboratory frame is treated approximately by considering only a few “principal” orientations.^{28, 43} The atomic selection rules are applied to each spherical harmonic contributing to the parent orbital to determine the allowed partial waves emitted for each principal orientation. The angular component of the photoelectron wave function resulting from each principal orientation is expressed as a coherent superposition of the allowed spherical harmonics. The angular distributions for different principal orientations are then combined incoherently, on the assumption that the timescale of rotation is long relative to the photodetachment timescale.

The specific object of this paper is to explicitly demonstrate this approach on the simplest case, that of a parent orbital represented as a combination of bound s and p functions (i.e., the angular part of the parent wave function is a linear combination of spherical harmonics for $\ell_i = 0$ and 1). In Sec. II, we construct an expression for the photoelectron anisotropy parameter in terms of fractional p character of the parent state, relative partial-wave cross sections, and the phase shift between different allowed photoelectron partial waves. We show that in the limits of pure s or pure p electron photodetachment or photoionization, the resulting expression reduces to the familiar Cooper–Zare formula.^{14, 15} Hence, the principal result of Sec. II is a generalization of the

Cooper–Zare equation for the case of mixed s and p state photodetachment (photoionization). In Sec. III, we compare the model predictions to experimental data for strongly solvated H^- and NH_2^- anions,⁴⁷ corresponding to the strongly perturbed, predominantly s and predominantly p parent states, respectively.

II. THE MODEL

A. Photodetachment/photoionization from a superposition of s and p states

We now build a one-electron model for photodetachment from a stationary state whose angular dependence may be expanded as a linear combination of one s- and one p-type function,

$$|\psi_i\rangle = \sqrt{1-f}|s\rangle + \sqrt{f}|p\rangle, \quad (4)$$

where f is the fractional p-character of the state ($0 \leq f \leq 1$). Any relative phase factors for the s and p contributions to $|\psi_i\rangle$ are absorbed into the corresponding kets. Moreover, without loss of generality, we define the direction of the p term in Eq. (4) as the molecular-frame z axis.

Similar to the initial (bound) state, we shall describe the free (emitted) electron as a superposition of partial waves with defined l values. In accordance with dipole selection rules, the s term in Eq. (4) will give rise to p partial waves, while the p term will yield s- and d-type partial waves. The laboratory-frame PAD depends upon the partial waves emitted for all possible orientations of the parent orbital. The net observed photoelectron probability distribution may be written as an incoherent superposition of the distributions resulting from principal orientations.²⁸

$$I(\theta) \approx I_X(\theta) + I_Y(\theta) + I_Z(\theta), \quad (5)$$

where subscripts X, Y, and Z indicate the orientations of the molecular frame relative to the laboratory frame, defined so that the molecular-frame quantization axis (z) is parallel to the laboratory-frame x, y, and z axes, respectively.

We set the direction of the light's electric field vector as the laboratory frame z axis and hereon define the projection quantum numbers for all emitted partial waves relative to this axis. Principal orientation Z corresponds to the p component of the parent orbital (Eq. (4)) aligned along z. Within the electric-dipole approximation, this orientation yields a $p_0 = p_z$ partial wave resulting from the s term in Eq. (4) and a combination of s and $d_0 = d_{z^2}$ partial waves resulting from the p term.

For orientations X and Y, the s component of the parent orbital also yields a p_z partial wave. The p term in Eq. (4) for these orientations transforms as laboratory-frame p_x and p_y functions, respectively. In terms of quantum numbers, these functions are linear combinations of $p_{\pm 1}$, which upon photodetachment yield $d_{\pm 1}$ partial waves. These transformations are summarized and illustrated graphically in Figure 1.

Using Eq. (1), we may express the photoelectron anisotropy parameter β as

$$\beta = \frac{\rho - 1}{1 + \rho/2}, \quad (6)$$

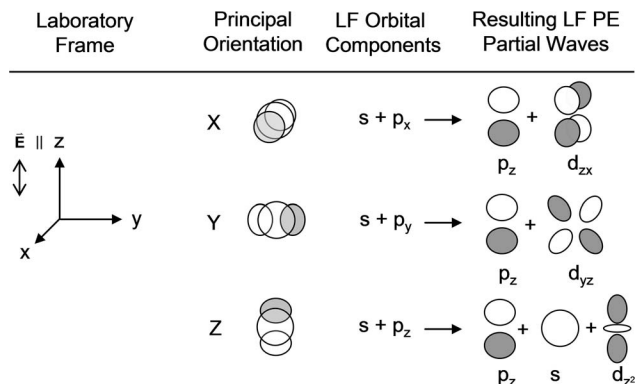


FIG. 1. Graphical representation of the partial-wave contributions from s and p parent orbital components for three principal orientation. See text for details.

where

$$\rho = \frac{I(0^\circ)}{I(90^\circ)}. \quad (7)$$

We therefore need only know the ratio of the photoelectron intensities at $\theta = 0^\circ$ and 90° in order to write an expression for β , and may neglect all terms in Eq. (5) with no contribution to $I(0^\circ)$ and $I(90^\circ)$.

In calculating the net orientation-averaged photoelectron intensities, to each principal orientation there corresponds an additional term resulting from the opposite direction of the molecular-frame z axis in the laboratory frame. Because the p wave has ungerade symmetry, while s and d_{z^2} waves are gerade, there is no net s–p or p–d interference. For these reasons, we consider only the original X, Y, and Z orientations and neglect the s– p_z and the p_z – d_{z^2} cross terms.

Referring to Figure 1 and making use of the axial symmetry of the s, p_z , and d_{z^2} functions with respect to the z axis, we may write:

$$I(\theta) = |\Psi(\theta)|^2 = |\sqrt{f}e^{i\delta_0}C_0Y_{00}(\theta) + \sqrt{f}e^{i(\delta_2+\pi)}C_2Y_{20}(\theta)|^2 + 3|\sqrt{1-f}e^{i(\delta_1+\pi/2)}C_1Y_{10}(\theta)|^2 + [d_{xz}, d_{yz} \text{ terms}], \quad (8)$$

where $Y_{\ell m}$ are the spherical harmonics and C_1 the coefficients for the corresponding partial waves. The coefficients are assumed proportional to the radial matrix elements $\chi_{\ell_i, \ell_i \pm 1}$ connecting the partial waves with the relevant components of the parent orbital, namely: $C_0 \propto \chi_{1,0}$, $C_1 \propto \chi_{0,1}$, and $C_2 \propto \chi_{1,2}$. The first square-modulus term in Eq. (8) accounts for the superposition of the s and d_{z^2} partial waves resulting from orientation Z. The net amplitudes of these waves are proportional to the amplitude of the p component of the parent orbital, \sqrt{f} , per Eq. (4). The second square-modulus term describes the contribution of the p_z waves resulting from each of the three (hence the factor 3 in front) principal orientations. The amplitude of each of these waves is proportional to the amplitude of the s component of the parent orbital, $\sqrt{1-f}$. The phase shifts of $\pi/2$ and π are due to interactions of the p and d waves (respectively) with the centrifugal barrier,⁴⁸ while δ_1 are additional phase shifts induced by interaction of the partial waves with the neutral fragment. The contributions of the d_{xz} , d_{yz} waves in Eq. (8) are not spelled out explicitly, because these

waves have nodes at both $\theta = 0^\circ$ and 90° ; moreover, we do not consider their interference with the s and d_{z^2} waves, because these waves are not emitted from the same principal orientations (see Figure 1).

Using Eq. (8) and the spherical-harmonics properties, we construct the parallel and perpendicular photoelectron intensities:

$$I(0^\circ) = |\sqrt{f}e^{i\delta_0}C_0Y_{00}(0^\circ) + \sqrt{f}e^{i(\delta_2+\pi)}C_2Y_{20}(0^\circ)|^2 + 3|\sqrt{1-f} \cdot e^{i(\delta_1+\pi/2)}C_1Y_{10}(0^\circ)|^2, \quad (9)$$

$$I(90^\circ) = |\sqrt{f}e^{i\delta_0}C_0Y_{00}(90^\circ) + \sqrt{f}e^{i(\delta_2+\pi)}C_2Y_{20}(90^\circ)|^2. \quad (10)$$

We arbitrarily define the spherical harmonics as unnormalized functions ($Y_{00} = 1$, $Y_{10} = \cos\theta$, $Y_{20} = 3\cos^2\theta - 1$), incorporating the necessary normalization constants in the coefficients C_i . Equations (9) and (10) may then be simplified to

$$\beta = \frac{2(1-f)(C_1/C_0)^2 + 2f(C_2/C_0)^2 - 4f(C_2/C_0)\cos(\delta_2 - \delta_0)}{f + 2f(C_2/C_0)^2 + (1-f)(C_1/C_0)^2}. \quad (14)$$

Due to the assumptions made along the way, this equation is approximate. However, in the limit of $f = 0$, it reduces to $\beta = 2$, as expected for detachment from a pure s orbital ($\ell_i = 0$). In the limit of $f = 1$, Eq. (14) similarly reduces to the Cooper-Zare expression (Eq. (2)) for photodetachment from a p orbital ($\ell_i = 1$), since $C_2/C_0 = \chi_{1,2}/\chi_{1,0}$. Hence, the general approach of the model seems to provide a simple, alternate way to arrive at the Cooper-Zare equation.

B. Application to anion photodetachment

The primary objective in developing this model has been to construct an analytical expression for the energy-dependence of photoelectron anisotropy parameters that may be fit to experimental data. For anions, the energy-dependence of β arises due to the energy-dependence of the relative partial-wave cross sections. Assuming, as before,²⁰ the Wigner-law²¹ scaling of the partial cross sections σ_ℓ , we may write:

$$\frac{C_1^2}{C_0^2} = \frac{\chi_{0,1}^2}{\chi_{1,0}^2} = \frac{\sigma_1}{\sigma_0} = B\varepsilon, \quad (15)$$

$$\frac{C_2^2}{C_0^2} = \frac{\chi_{1,2}^2}{\chi_{1,0}^2} = \frac{\sigma_2}{\sigma_0} = A^2\varepsilon^2, \quad (16)$$

where A and B are constants. Substituting Eqs. (15) and (16) into (14) yields β as an explicit function of electron kinetic

$$I(0^\circ) = fC_0^2 + 3(1-f)C_1^2 + 4fC_2^2 - 4fC_0C_2\cos(\delta_2 - \delta_0), \quad (11)$$

$$I(90^\circ) = fC_0^2 + fC_2^2 + 2fC_0C_2\cos(\delta_2 - \delta_0). \quad (12)$$

The absence of δ_1 in Eqs. (11) and (12) reflects the lack of net interference between the $\ell = 1$ partial waves and the $\ell = 0, 2$ waves. Substituting Eqs. (11) and (12) into Eq. (7) yields

$$\rho = \frac{fC_0^2 + 3(1-f)C_1^2 + 4fC_2^2 - 4f \cdot C_0C_2\cos(\delta_2 - \delta_0)}{fC_0^2 + fC_2^2 + 2fC_0C_2\cos(\delta_2 - \delta_0)}. \quad (13)$$

And finally, substituting Eq. (13) into Eq. (6) and dividing both the numerator and the denominator of the resulting fraction by C_0^2 gives

energy:

$$\beta = \frac{2(1-f)B\varepsilon + 2fA^2\varepsilon^2 - 4fA\varepsilon\cos(\delta_2 - \delta_0)}{f + 2fA^2\varepsilon^2 + (1-f)B\varepsilon}. \quad (17)$$

This is the main result of the model. It differs from the WBCZ model (Eq. (3)) in that it describes photodetachment from a mixed sp orbital. We expect that the approach of the model can be readily generalized for other types of mixed parent states. Although several approximations have been made in the derivation of Eq. (17), the overall approach is non-perturbative, as no assumptions are made about the magnitude of the net p-character of the parent state, $0 \leq f \leq 1$. In the two limiting cases, $f = 0$ and $f = 1$, Eq. (17) reduces exactly to the respective WBCZ predictions for detachment from s and p orbitals. Constant A in Eq. (17) has the same meaning as in Eq. (3),²⁰ while parameter B is newly introduced here, in order to similarly describe the relative scaling of the $\ell = 1$ and $\ell = 0$ cross sections.

For the purpose of illustration, in Figure 2, we arbitrarily assumed $A = B$ and plotted β (as given by Eq. (17)) as a function of $A\varepsilon$ ($= B\varepsilon$) for several values of f ranging from 0 to 1. We note that β always approaches 0 in the limit of $\varepsilon \rightarrow 0$, as long as $f \neq 0$. That is the s waves dominate, no matter how small the net p-character of the parent state.

III. COMPARISON TO EXPERIMENT

Equation (17) may be used to model experimental data for photodetachment from a system that may be approximated

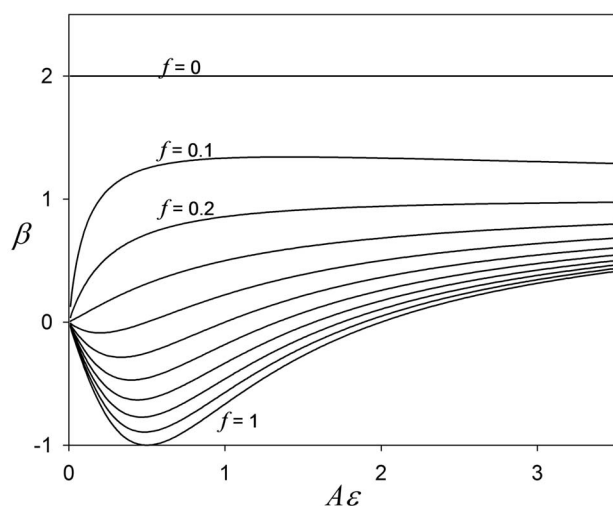


FIG. 2. Energy dependence of the anisotropy parameter for photodetachment from mixed sp states, as given by Eq. (17) for different values of f between 0 and 1 in increments of 0.1, assuming $A = B$ and $\delta = 0$. For example, if $A = 1 \text{ eV}^{-1}$, the horizontal axis corresponds to ϵ in eV.

as a linear superposition of bound s and p functions. The H^- and NH_2^- anions, respectively, solvated by ammonia, are excellent trial systems for this model. In the accompanying paper,⁴⁷ we reported our recent experimental results for the $\text{H}^-(\text{NH}_3)_n$ and $\text{NH}_2^-(\text{NH}_3)_n$ cluster anions. Here, we use the formalism developed in Sec. II to model the PADs observed in the photodetachment of these strongly solvated ions.

In the first example (Sec. III A), electron emission from $\text{H}^-(\text{NH}_3)_n$ involves strongly perturbed, but predominantly s parent states. We approximate the solvation effects on the ground state of H^- by adding a p polarization term to the parent s orbital (via Eq. (4)) and apply the model (Eq. (17)) in the regime of small (but not necessarily perturbatively small) f . In the second case (Sec. III B), the HOMO of NH_2^- is a non-bonding p orbital localized on the nitrogen atom. Solvation by ammonia breaks the orbital symmetry and thus affects the PAD. In Sec. III B, we attempt to describe this effect by adding an opposite-symmetry s term to the parent state, utilizing Eqs. (4) and (17) with large (close to 1) values of f .

A. Solvated H^- : Polarized s state photodetachment

In an isotropic environment, the electron density in the hydride anion is spherically symmetric. In the photodetachment from the $1s$ orbital of H^- , only $\ell = 1$ waves are allowed. Accordingly, the Cooper-Zare model (Eq. (2)) and, by extension, the WBCZ equation (Eq. (3)) predict $\beta = 2$, independent of photon wavelength or electron kinetic energy.

The presence of solvent breaks the spherical symmetry, resulting in the lifting of some angular-momentum restrictions on the partial waves emitted in electron photodetachment. In particular, $\ell = 0$ partial waves may become dipole-allowed in the photodetachment of $\text{H}^-(\text{X})_n$ cluster anions, where X is arbitrary solvent. The opening of the $\ell = 0$ channel has a profound effect on the PADs, particularly at small ϵ , where s waves are expected to dominate over $\ell = 0$ contributions,²⁴ as prescribed by the Wigner law.²¹

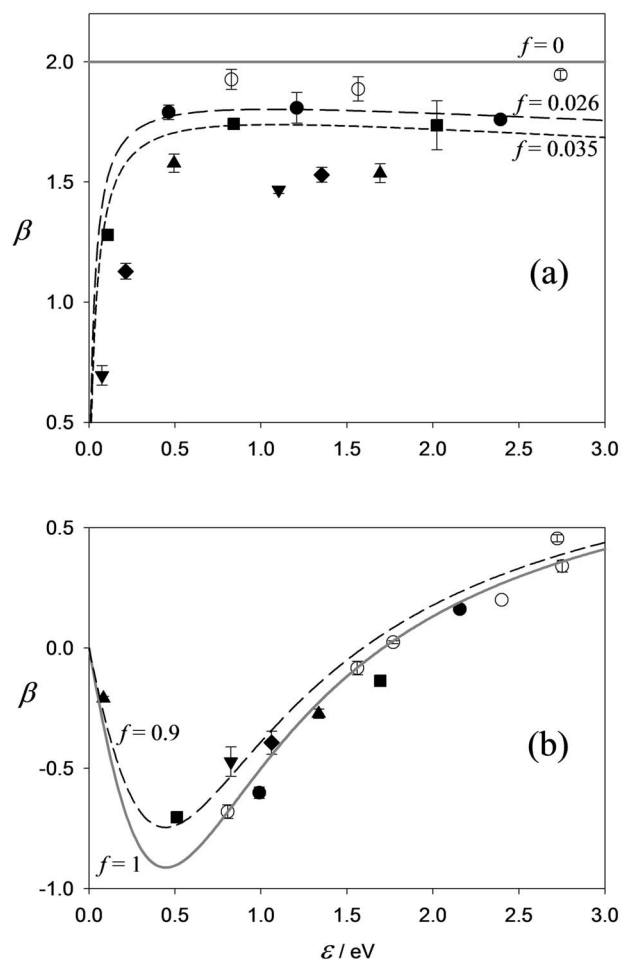


FIG. 3. Experimental (symbols) energy-dependence of photoelectron anisotropy parameters for photodetachment from (a) $\text{H}^-(\text{NH}_3)_n$, $n = 0-5$ at 532 and 355 nm, $n = 0-2$ at 786 nm (data from Ref. 47) and (b) $\text{NH}_2^-(\text{NH}_3)_n$, $n = 0-5$ at 532 and 355 nm, $n = 0$ at 786, 488, and 351 nm (data from Refs. 47, 49, 50). Lines correspond to predictions of the current model (Eq. (17)) for indicated values of f . See text for details.

This effect is clearly borne out in our photoelectron imaging data for $\text{H}^-(\text{NH}_3)_n$, $n = 1-5$ cluster ions,⁴⁷ included here in Figure 3(a), where the observed β values deviate drastically from the Cooper-Zare prediction of $\beta = 2$, particularly at small ϵ .

To model this effect, we first turn to the $\text{H}^-(\text{NH}_3)$ cluster anion, in which the solvent-induced perturbation of the $1s$ orbital of H^- may be approximated as a charge-dipole interaction polarizing the orbital along the interaction axis. The perturbed orbital, lacking inversion symmetry, must be described as a linear combination of even and odd functions, so we combine the initial s orbital of H^- with a p -type function polarized along the direction of the interaction (Eq. (4)).

We have plotted the prediction of our model (Eq. (17)) for $f = 0.026$ (solid grey curve) and 0.035 (dashed grey curve) in Figure 3(a). As the phase shift between the $\ell = 0$ and 2 partial waves is typically small for atomic anion photodetachment, $\cos(\delta_2 - \delta_0)$ has been set to 1; we have also arbitrarily set $A = B = 1 \text{ eV}^{-1}$. The model result qualitatively agrees with the experimentally determined trends in β for $\text{H}^-(\text{NH}_3)_n$, $n = 1-5$ cluster ions. In fact, the two plotted curves overlap

quite well with the experimental data for $\text{H}^-(\text{NH}_3)$ and $\text{H}^-(\text{NH}_3)_2$, respectively. Most importantly, the model correctly predicts the rapid decrease in photoelectron anisotropy with decreasing ε —the effect that the WBCZ model cannot account for.

We note that any number of solvent molecules could be viewed as introducing additional p-components in the parent orbital at different positions relative to the first, depending on the cluster geometry. Considering all relevant orientations of these additional components would yield additional s and d partial-waves. However, the value of f in Eq. (4) does not necessarily increase with increasing n . The p polarization term in this case can be regarded as a measure of solvation asymmetry, which is expected to become small as the first solvation shell is completed.

The approximation of the parent orbital as a linear combination of s and p states is likely to become less rigorous for the $\text{H}^-(\text{NH}_3)_n$, $n > 1$ clusters. However, $\ell = 0$ partial waves resulting from any solvation-induced p character in the parent orbital will always dominate over partial-waves with larger ℓ values at small ε , resulting in decreasing β values as $\varepsilon \rightarrow 0$.

B. Solvated NH_2^- : Perturbed p state photodetachment

We now consider the photoelectron angular distributions for solvated NH_2^- by comparing the model prediction to the photoelectron imaging results for $\text{NH}_2^-(\text{NH}_3)_n$, $n = 1-5$ cluster anions, included in Figure 3(b).⁴⁷ The non-bonding b_1 HOMO of unsolvated NH_2^- is essentially a p orbital on the nitrogen atom. Upon solvation, the electron density within the anion should be perturbed along the solvent-ion interaction axis, in general breaking the ungerade symmetry of the orbital. The effect may be described by adding gerade perturbation terms to the original p function. For most solvation geometries, the first term in the perturbation expansion is likely to be an s-like function. Under this approximation, we may also use Eq. (17) to model β vs. ε for photodetachment from solvated NH_2^- , treating the parent orbital as a p orbital with some s character (Eq. (4) with f close to 1).

The model prediction for $f = 0.90$ is plotted in Figure 3(b) as a dashed line, again assuming $A = B$ and using the parameters determined for bare NH_2^- : $A = 1.09 \text{ eV}^{-1}$ and $\cos(\delta_2 - \delta_0) = 0.934$.⁴⁷ The model prediction compares favorably with the experimental data; however, it is not too different from the prediction of the unmodified ($f = 1$) WBCZ model (grey curve in Figure 3(b)).

Overall, perturbation alters the $\beta(\varepsilon)$ dependence resulting from a predominantly p parent state to a smaller degree than for s-orbital photodetachment. This conclusion may be understood by considering that in pure s state photodetachment, only $\ell = 1$ waves are allowed, corresponding to the theoretical WBCZ limit of $\beta = 2$. Addition of any p character to the parent state opens the $\ell = 0$ channel, which, due to the Wigner law, dominates the photodetachment process at small-to-moderate ε .^{21,24} To the contrary, in p state photodetachment, addition of some s character to the initial state leads to the opening of the $\ell = 1$ channel, which, by the same logic, does not compete favorably with the $\ell = 0$ waves emitted from the unperturbed p state.

IV. SUMMARY

We have presented a simple non-perturbative approach to modeling photoelectron angular distributions for photodetachment or photoionization from a mixed sp state. We derived an analytical expression for the energy-dependence of the photoelectron anisotropy parameter, β , for the case of photodetachment, which includes parametric dependence on the fractional p character on the parent state. The predictions of the model are compared to experimental results for solvated H^- and NH_2^- and the model is found to be in agreement with experiment.

ACKNOWLEDGMENTS

This work was supported by the U.S. National Science Foundation (Grant No. CHE-1011895).

- ¹A. Sanov and R. Mabbs, *Int. Rev. Phys. Chem.* **27**, 53 (2008).
- ²D. W. Chandler and P. L. Houston, *J. Chem. Phys.* **87**, 1445 (1987).
- ³A. J. R. Heck and D. W. Chandler, *Annu. Rev. Phys. Chem.* **46**, 335 (1995).
- ⁴A. Eppink and D. H. Parker, *Rev. Sci. Instrum.* **68**, 3477 (1997).
- ⁵J. H. D. Eland, *Photoelectron Spectroscopy: An Introduction to Ultraviolet Photoelectron Spectroscopy in the Gas Phase* (Butterworths, London, 1984).
- ⁶K. M. Ervin and W. C. Lineberger, in *Advances in Gas Phase Ion Chemistry*, edited by N. G. Adams and L. M. Babcock (JAI, Greenwich, 1992), Vol. 1, p. 121.
- ⁷P. Lin and R. R. Lucchese, *J. Chem. Phys.* **114**, 9350 (2001).
- ⁸T. Seideman, *Annu. Rev. Phys. Chem.* **53**, 41 (2002).
- ⁹K. L. Reid, *Annu. Rev. Phys. Chem.* **54**, 397 (2003).
- ¹⁰C. M. Oana and A. I. Krylov, *J. Chem. Phys.* **131**, 124114 (2009).
- ¹¹V. Blanchet, M. Z. Zgierski, and A. Stolow, *J. Chem. Phys.* **114**, 1194 (2001).
- ¹²M. Schmitt, S. Lochbrunner, J. P. Shaffer, J. J. Larsen, M. Z. Zgierski, and A. Stolow, *J. Chem. Phys.* **114**, 1206 (2001).
- ¹³J. Cooper and R. N. Zare, in *Atomic Collision Processes*, edited by S. Geltman, K. T. Mahanthappa, and W. E. Brittin (Gordon and Breach, New York, 1968), Vol. XI-C, p. 317.
- ¹⁴J. Cooper and R. N. Zare, *J. Chem. Phys.* **48**, 942 (1968).
- ¹⁵J. Cooper and R. N. Zare, *J. Chem. Phys.* **49**, 4252 (1968).
- ¹⁶H. A. S. Bethe and E. E. Salpeter, *Quantum Mechanics of One- and Two-Electron Atoms* (Springer-Verlag/Academic, Berlin/New York, 1957).
- ¹⁷M. A. Sobhy and A. W. Castleman, *J. Chem. Phys.* **126**, 154314 (2007).
- ¹⁸G. Aravind, N. B. Ram, A. K. Gupta, and E. Krishnakumar, *Phys. Rev. A* **79**, 043411 (2009).
- ¹⁹A. M. Covington, S. S. Duvvuri, E. D. Emmons, R. G. Kraus, W. W. Williams, J. S. Thompson, D. Calabrese, D. L. Carpenter, R. D. Collier, T. J. Kvale, and V. T. Davis, *Phys. Rev. A* **75**, 022711 (2007).
- ²⁰D. Hanstorp, C. Bengtsson, and D. J. Larson, *Phys. Rev. A* **40**, 670 (1989).
- ²¹E. P. Wigner, *Phys. Rev.* **73**, 1002 (1948).
- ²²W. C. Lineberger, H. Hotop, and T. A. Patterson, in *Electron and Photon Interactions with Atoms*, edited by H. Kleinpoppen and M. R. C. McDowell (Plenum, New York, 1976), p. 125.
- ²³R. D. Mead, K. R. Lykke, and W. C. Lineberger, in *Electronic and Atomic Collisions*, edited by J. Eichler, I. V. Hertel, and N. Stolterfoht (Elsevier, New York, 1984), pp. 721.
- ²⁴K. J. Reed, A. H. Zimmerman, H. C. Andersen, and J. I. Brauman, *J. Chem. Phys.* **64**, 1368 (1976).
- ²⁵J. R. Smith, J. B. Kim, and W. C. Lineberger, *Phys. Rev. A* **55**, 2036 (1997).
- ²⁶J. B. Kim, P. G. Wenthold, and W. C. Lineberger, *J. Chem. Phys.* **108**, 830 (1998).
- ²⁷W. D. Brandon, D. H. Lee, D. Hanstorp, and D. J. Pegg, *J. Phys. B* **31**, 751 (1998).
- ²⁸E. Surber, R. Mabbs, and A. Sanov, *J. Phys. Chem. A* **107**, 8215 (2003).
- ²⁹R. Mabbs, E. Surber, and A. Sanov, *J. Chem. Phys.* **122**, 054308 (2005).
- ³⁰S. J. Cavanagh, S. T. Gibson, M. N. Gale, C. J. Dedman, E. H. Roberts, and B. R. Lewis, *Phys. Rev. A* **76**, 052708 (2007).
- ³¹L. Velarde, T. Habteyes, E. R. Grumbling, K. Pichugin, and A. Sanov, *J. Chem. Phys.* **127**, 084302 (2007).

- ³²G. Aravind, A. K. Gupta, M. Krishnamurthy, and E. Krishnakumar, *Phys. Rev. A* **75** (2007).
- ³³C. M. Oana and A. I. Krylov, *J. Chem. Phys.* **127**, 234106 (2007).
- ³⁴M. Van Duzor, J. Wei, F. Mbaiwa, and R. Mabbs, *J. Chem. Phys.* **131**, 204306 (2009).
- ³⁵F. Mbaiwa, J. Wei, M. Van Duzor, and R. Mabbs, *J. Chem. Phys.* **132**, 134304 (2010).
- ³⁶R. Mabbs, F. Mbaiwa, J. Wei, M. Van Duzor, S. T. Gibson, S. J. Cavanagh, and B. R. Lewis, *Phys. Rev. A* **82**, 011401 (2010).
- ³⁷M. Van Duzor, F. Mbaiwa, J. Wei, T. Singh, R. Mabbs, A. Sanov, S. J. Cavanagh, S. T. Gibson, B. R. Lewis, and J. R. Gascooke, *J. Chem. Phys.* **133**, 174311 (2010).
- ³⁸M. A. Sobhy, K. Casalenuovo, J. U. Reveles, U. Gupta, S. N. Khanna, and A. W. Castleman, *J. Phys. Chem. A* **114**, 11353 (2010).
- ³⁹E. R. Grumbling, K. Pichugin, L. Velarde, and A. Sanov, *J. Phys. Chem. A* **114**, 1367 (2010).
- ⁴⁰R. N. Zare, *Mol. Photochem.* **4**, 1 (1972).
- ⁴¹T. Seideman, *J. Chem. Phys.* **107**, 7859 (1997).
- ⁴²J. G. Underwood and K. L. Reid, *J. Chem. Phys.* **113**, 1067 (2000).
- ⁴³E. Surber and A. Sanov, *J. Chem. Phys.* **116**, 5921 (2002).
- ⁴⁴H. Tomioka, *Acc. Chem. Res.* **30**, 315 (1997).
- ⁴⁵R. L. Schwartz, G. E. Davico, T. M. Ramond, and W. C. Lineberger, *J. Phys. Chem. A* **103**, 8213 (1999).
- ⁴⁶D. J. Goebbert, K. Pichugin, D. Khuseynov, P. G. Wenthold, and A. Sanov, *J. Chem. Phys.* **132**, 224301 (2010).
- ⁴⁷E. R. Grumbling and A. Sanov, *J. Chem. Phys.* **135**, 164301 (2011).
- ⁴⁸R. Mabbs, E. R. Grumbling, K. Pichugin, and A. Sanov, *Chem. Soc. Rev.* **38**, 2169 (2009).
- ⁴⁹R. J. Celotta, R. A. Bennett, and J. L. Hall, *J. Chem. Phys.* **60**, 1740 (1974).
- ⁵⁰C. T. Wickham-Jones, K. M. Ervin, G. B. Ellison, and W. C. Lineberger, *J. Chem. Phys.* **91**, 2762 (1989).